Conf-920212--2
58918-00-105 February 1992

Manuscript

ANL/CP--75618
DE92 009726

MAGNETO-OPTICAL MULTILAYERS*

S.D. Bader

Materials Science Division
Argonne National Laboratory, Argonne, IL 60439

INVITED PAPER: Optical Data Storage '92 Topical Meeting, February 9-13, 1992, San Jose, CA.

jmc

*Work supported by the U.S. Department of Energy under contract #W-31-109-ENG-38.

Magneto-optic multilayers

S. D. Bader

Materials Science Division, Argonne National Laboratory, Argonne, IL 60439

ABSTRACT

Magneto-optical multilayers are of interest to the optical data storage community as a possible second-generation medium of the future. The important Co/Pt-superlattice system is introduced in this respect, and an extensive reference listing is provided to previous research. Magneto-optical modeling studies of Co/Pt are presented, and it is concluded that the interfacial Pt is magnetized and is magneto-optically active at the short wavelengths of interest (~4 eV) for applications. Magneto-optics in the ultrathin limit are discussed, and an additivity law is presented and verified experimentally utilizing data for epitaxial Fe/Ag(111) superlattices. Finally, the surface magnetic anisotropy that provides the vertical easy axes of magnetization in candidate superlattice systems is discussed and illustrated experimentally using ultrathin epitaxial films of Fe grown on a variety of substrates. It is concluded that magneto-optic multilayers will provide many stimulating basic and applied challenges in the years ahead.

1. INTRODUCTION

First-generation magneto-optical media that are on the market today consist of amorphous rare-earth-transition-metal alloy films that are overcoated and undercoated to enhance their magnetic, optical, tribological, and corrosion-resistant properties.[1] The magneto-optic multilayers of interest in the present context, however, consist not of a single magneto-optically active film, but of a repetitive sequence of ultrathin (nanometer-scale) layers that can form a superlattice.[2] This composite multilayer stack can then be similarly overcoated and undercoated.[3] Interest in such multilayers was first stimulated by reports that Co/Pt superlattices are candidate materials for second-generation magneto-optic media.[4,5] Co/Pt potentially offers higher-density information storage than conventional media because of its favorable response at shorter wavelengths. It also has a higher corrosion resistance than rare-earth-containing media. A typical composition of interest is $[Co(4Å)/Pt(13Å)]_n$, where n~10 repetitions lead to a total superlattice thickness comparable to the depth penetration of the incident light. Interest in Co/Pt subsequently blossomed[6] and includes the characterization of polycrystalline multilayers fabricated by sputtering[7] and evaporation[8] techniques,[9] as well as epitaxially oriented multilayers grown in ultrahigh vacuum using molecular-beam-epitaxy growth techniques.[10] Recent work also includes experimental studies of related systems, such as Co/Pd[11] and Co/Cu,[12] and analyses of their behavior by magneto-optic modeling approaches[13,14] and by electronic structure calculations.[15,16]

The purpose of the present work is as follows: Firstly, to acquaint the reader with magneto-optic modeling studies for Co/Pt superlattices. Secondly, to discuss the underlying physics that makes Co/Pt such an interesting system. Two of the key features are (i) the polarizability and magneto-optic activity of the interfacial Pt, and (ii) the perpendicular surface or interfacial magnetic anisotropy of the ultrathin Co layers. Favorable magneto-optical properties are achieved in the Co/Pt system because the epitaxy and the quality of the interfaces can be adjusted quite readily to allow these two features to manifest themselves. Finally, examples are presented of related systems that illustrate the features of interest.

2. MAGNETO-OPTICS FORMALISM

In this section the macroscopic Kerr-effect formalism of Zak *et al.* is preseneted.[17] The choice of formalism is dictated by the interests and familiarity of the author. Insights will then be obtained by considering the ultrathin limit, and examining instructive simulations and measurements.

A beam of light travelling from medium 1 to medium 2 conserves the tangential components of its electric E_x, E_y and magnetic H_x, H_y fields, where the xy-plane is the boundary between the two media. Expressed in terms of the electric fields of the incident (i) and reflected (r) waves we can write

$$F = \begin{pmatrix} E_x \\ E_y \\ H_x \\ H_y \end{pmatrix} = A\,P = A \begin{pmatrix} E_s^{(i)} \\ E_p^{(i)} \\ E_s^{(r)} \\ E_p^{(r)} \end{pmatrix} ,$$

where the 4x4 matrix A that connects column vectors F and P is called the *medium boundary matrix.* The matrix elements of A are constructed from the geometric angles of the problem and from the N and Q-values of the medium, where N is the index of refraction and Q is the magneto-optic (Voigt) coupling constant. For a two-medium, one-boundary problem, the boundary matching condition becomes

$$A_1 P_1 = A_2 P_2 .$$

If there is more than one boundary, the wave propagation inside the medium at depth z from the interface is described using the *medium propagation matrix* $\overline{D}$, where

$$P_2(z=0) = \overline{D}_2(z)\, P_2(z) .$$

For a multilayer system, the light originates in the initial medium i, goes through the multilayer stack, and ends up in the substrate or final medium f. The information of interest for l layers in the stack is contained in the expression

$$A_i P_i = \prod_{m=1}^{l} (A_m \overline{D}_m A_m^{-1})\, A_f P_f .$$

If we put this expression in the form $P_i = M P_f$, where

$$M = A_i^{-1} \prod_m A_m \overline{D}_m A_m^{-1}\, A_f \equiv \begin{pmatrix} G & H \\ I & J \end{pmatrix} ,$$

then the 2x2 matrices G and I can be used to obtain the Fresnel transmission t and reflection coefficients, since

$$G^{-1} = \begin{pmatrix} t_{ss} & t_{sp} \\ t_{ps} & t_{pp} \end{pmatrix} \quad \text{and} \quad IG^{-1} = \begin{pmatrix} r_{ss} & r_{sp} \\ r_{ps} & r_{pp} \end{pmatrix} .$$

The Kerr rotation ϕ' and ellipticity ϕ'' for s- and p-polarized light are then expressed as:

$$\phi_s = \phi'_s + i\,\phi''_s = \frac{r_{ps}}{r_{ss}} \quad \text{and} \quad \phi_p = -\phi'_p + i\,\phi''_p = \frac{r_{sp}}{r_{pp}} .$$

Prescriptions for constructing the A and $\overline{D}$ matrices appear in Ref. 17.

3. THE ULTRATHIN LIMIT

The formal expressions above simplify and provide useful insights in the ultrathin limit, which is defined by

$$\frac{2\pi}{\lambda} |N|\, d << 1 ,$$

where λ is the wavelength of the light and d is the thickness in Å of the film.[16] In the ultrathin limit for a magnetic overlayer, characterized by N, Q and d, on a non-magnetic substrate with refractive index N_{sub}, the polar (POL) and longitudinal (LON) Kerr effects become:

$$\phi^{POL} = -\left(\frac{4\pi}{\lambda}\right)\left(\frac{N^2}{1-N_{sub}^2}\right) Q\, d \quad \text{and} \quad \phi^{LON} = \left(\frac{4\pi}{\lambda}\right)\left(\frac{N_{sub}}{1-N_{sub}^2}\right) \theta\, Q\, d \;, \tag{1}$$

where θ, the angle of incidence measured from the surface normal, is assumed small. For a multilayer stack in the ultrathin limit there is an additivity law whereby the total ϕ^{POL} and ϕ^{LON} are represented by the appropriate expressions in Eq. 1 summed over the magnetic layers: $\phi_{total} = \Sigma\phi$. Also, Eq. 1 illustrates that $\phi^{POL} >> \phi^{LON}$ because of the extra N-factor and the lack of a θ-factor in ϕ^{POL}. Note that ϕ^{LON} is independent of the refractive index of the magnetic layer. This implies that ϕ^{LON} can be enhanced by choosing a substrate with an appropriate value of N_{sub}.

Additional insights comes from consideration of superlattices (SL) of magnetic and non-magnetic layers of thicknesses d_1 and d_2, respectively, that satisfy the ultrathin criterion. It can be shown that if $N_1 \sim N_2$, as is the case for Co and Pt in the vicinity of 2-eV photon energy, there is a remarkably simple relationship to the Kerr effect of bulk films:[18]

$$\frac{\phi_{SL}}{\phi_{bulk}} = \frac{d_1}{d_1 + d_2} \;. \tag{2}$$

4. SIMULATIONS

Figure 1 shows experimental polar Kerr-effect data for Co/Pt superlattices, taken from Zeper *et al.*,[4] compared to simulations that utilize the full formalism of the previous section.[14] Tabulated optical constants[19] and Q-values[20] were used in the simulation. The experimental data for the superlattices show the enhanced rotation at 4-eV photon energy compared to that for bulk Co. The simulations fail to show the enhancement, but instead show the scaling behavior with Co thickness embodied in Eq. 2. Similar comparisons of experiment and simulations for Co/Pd and Co/Cu superlattices show better agreement than for the Co/Pt system.[14] The reason for the discrepancy between experiment and simulation in the Co/Pt case is attributed to the magneto-optic activity of the interfacial Pt. In the simulation the Q value of Pt is taken to be zero, as is the case for the bulk material. However, it is well known that Pt or Pd layers in proximity to magnetic 3*d* elements acquire a small magnetic moment. The magneto-optic activity is related to the moment *and* to the magneto-optic matrix element that is due to the spin-orbit interaction. We believe that the magneto-optic activity of Pt can be particularly large because spin-orbit effects become increasingly important for heavier elements. The importance of the Pt contribution at 4 eV is presumably associated with the total spin polarization of the bottom of the Pt *d* band, which should be ~4eV below the Fermi energy. These ideas are discussed further in Refs. 6 and 13-16. Comparisons between simulations for the longitudinal Kerr effect and experiment appear in the literature also for Fe overlayers[21] on Au(100), and for Fe/Cr,[22] Fe/Mo,[23] Fe/Nb,[24] Fe/Ag,[25] and Co/Cu[26] superlattices.

The simulations in Ref. 13 for the polar Kerr effect of Co/Pt superlattices are particularly all-inclusive, and were performed as a function of d_{Co} and d_{Pt}, the number of bilayers in the superlattice, the photon energy, angle of incidence, light polarization, and the refractive index of the substrate. The role of antireflection ZnS coatings in enhancing the Kerr effect at select wavelengths was also explored. Calculated under these various conditions were the rotation, ellipticity, reflectivity R, and ϕ_m, and the figure of merit $[(\phi_m)^2R]$ which represents the rotating power of the film. The quantity $\phi_m=[(\phi')^2+(\phi'')^2]^{1/2}$ is known as the magnitude of the complex rotation. Some of this information is reproduced in Fig. 2. The versatility of the simulation scheme suggests the possibility of computer-designing materials with optimized magneto-optical properties. However, the experimental properties of Co/Pt superlattices differ from the simulations because of the strong magneto-optic response from the interfacial Pt, due to its induced moments and large spin-orbit coupling. For example, we learn from the comparison that the choice of ~4Å of Co and ~13Å of Pt is *not* related to the optimization of the magneto-optic response. These thickness values are dictated by the requirement that the easy axes of magnetization be perpendicular to the plane of the film. For d_{Co} values that are much greater than ~4Å, the shape anisotropy overcomes the surface magnetic anisotropy and the easy axes are in-plane. The importance of perpendicular or vertical easy axes is that vertical media are believed to permit higher bit-packing densities than longitudinal media, due to their favorable demagnetization energetics for neighboring bits that are oppositely oriented. Also, the polar Kerr effect is the strongest and, therefore, most useful of the three Kerr effects (polar, longitudinal and transverse).

5. ADDITIVITY LAW FOR ULTRATHIN SUPERLATTICES

As was mentioned above, in the ultrathin limit the Kerr signal can be expressed as a sum over the individual contributions from each magnetic layer. This is illustrated in Fig. 3 for the case of epitaxial Fe(110)/Ag(111) superlattices grown by molecular beam epitaxy.[25] The longitudinal Kerr ellipticity at the He-Ne wavelength (1.96 eV) is plotted for different superlattice periodicities, and for increasing numbers of bilayers, n, in the superlattice. Each superlattice follows a separate curve when the data are plotted as a function of the total Fe/Ag film thickness, $n(d_{Fe}+d_{Ag})$. However, when the data are plotted as a function of the total Fe thickness, nd_{Fe}, all superlattices initially follow the same curve, as expected from the additivity law. Comparison between experiment and simulation, as displayed in the left and right panels of Fig. 3, respectively, permits the value of the Q parameter to be assessed. Recall that in the simulation the Q values are taken from the literature.[20] For the case of Fe/Ag the experimental and literature value of Q at 1.96 eV are found to be in remarkably good agreement. If the initial slopes associated with the additivity regime are compared, as displayed in the lower panels of Fig. 3, and it is assumed that all differences are attributed to Q as opposed to N, then there is agreement to the 5% level. Similar comparisons are presently underway for the Co/Cu system.[26] The reason for using Ag or Cu in these studies, rather than Pt or Pd, is to choose systems for which there is no significant interfacial polarization. That way the magneto-optic properties of the traditional magnetic element can be assessed more unambiguously. Significant differences are emerging in the Co/Cu comparison that suggest that the literature Q value for Co has less utility for our purposes than did the Q value for Fe. This work is presently underway and should be of interest in furthering our insights into the Co/Pt system.

6. VERTICAL SURFACE MAGNETIC ANISOTROPY IN ULTRATHIN FILMS

One of the key features of interest in Co/Pt superlattices is the vertical easy axes of magnetization for ultrathin Co-layer thicknesses. This anisotropy differs from that of the amorphous rare earth-transition metal media.[1,6] The vertical magnetic anisotropy of ultrathin films is related to the surface magnetic anisotropy first introduced by Néel, as is discussed by Gradmann.[27] The origin of the surface magnetic anistropy is due to the change in the spin-orbit-coupling energetics associated with the lowered symmetry at the surface relative to the bulk crystal. Fig. 4 shows a number of examples of vertical easy axes reorienting to in-plane easy axes as the film thickens, for epitaxial Fe films grown in ultrahigh vacuum onto a variety of single-crystalline substrates. The data in Fig. 4 were taken by means of *in-situ* magneto-optic Kerr-effect measurements. This approach has been dubbed with the acronym SMOKE, to stand for the surface magneto-optic Kerr effect.[28] The height of the Kerr loop in remanence is measured in arbitrary units. Typically, the maximum possible polar Kerr rotation value is ~0.1-0.2 mrad for an Fe monolayer. Initially the polar Kerr effect gives rise to remanent loops because the easy axes are vertical. Beyond a critical thickness d_c the easy axes are in-plane, and the remanent signal appears in the longitudinal Kerr effect. The polar and longitudinal signals are represented by square and triangular symbols, respectively. The polar signal is much stronger than the longitudinal signal, as expected.[28] Also shown in the panels on the right of Fig. 4 are the coercivities H_c of the films. While the H_c values are low for information-storage applications, they do tend to peak in the monolayer range where the strongest surface effects are expected. Detailed discussion and background material on these measurements and systems can be found in the literature.[28,29] An interesting aspect of the systems presented in Fig. 4 is that they represent phases that are stabilized by epitaxy. For example, while Fe is lattice matched to grow on Au(100) in its ordinary body-centered-cubic phase, Fe grows on Cu(100) in its face-centered-cubic (fcc) form, which is otherwise only stable in the bulk phase diagram at elevated temperatures. Fe grows on Pd(100) in a body-centered tetragonal phase that has no analogue in the bulk phase diagram. Thus, the importance of epitaxy is that it can be used to create new materials with interesting properties.

In the case of Co/Pt superlattices either the fcc or hexagonal close-packed phases are possibilities. The (111) texturing of the Pt template layer is believed to initially stabilize fcc-Co(111) layers. Also, the mismatch in lattice constants between Pt and Co introduce interfacial strain into the structure. The importance of these factors governs the useful thicknesses of the individual Co and Pt layers. Magneto-optically it would seem advantageous to increase the Co-layer thickness and decrease the Pt-layer thickness so that $d_{Co}>d_{Pt}$; but from the point of view of epitaxy and anisotropy the conditions $d_{Co}<<d_{Pt}$ are required. These type of considerations are brought out in the single-crystalline work presented in Ref. 10. Quite interestingly, the most practical consideration for there to be interest in Co/Pt multilayers stems from its corrosion resistance

as well as its magnetic or magneto-optic properties. It is anticipated that magneto-optic multilayers will provide many basic and applied challenges in the years ahead. This class of materials provides a fertile ground for 'atomically engineering' properties via artificial layering to create new structures.

7. ACKNOWLEDGMENTS

Work supported by U. S. Department of Energy, Basic Energy Sciences-Materials Sciences, under Contract #W-31-109-ENG-38. I thank my colleagues C. Liu, E. R. Moog, J. Pearson, Q. Qiu, and J. Zak for their help.

8. REFERENCES

1. B. S. Krusor and G. A. N. Connell, "Thin-film rare earth-transitional metal alloys for magnetooptic recording," *Physics of Thin Films*, edited by M. H. Franscombe and J. L. Vossen, Vol. 15, pp. 143-217 (Academic, Boston, 1991).

2. P. F. Carcia, A. Suna, D. G. Onn, and R. van Antwerp, "Structural, magnetic, and electrical properties of thin film Pd/Co layered structures," Superlattices and Microstructures, vol.1 (2), pp. 101-109, 1985.

P. F. Carcia, A. D. Meinhaldt, and A. Suna, "Perpendicular magnetic anisotropy in Pd/Co thin film layered structures," Appl. Phys. Lett., vol. 47 (2), pp. 178-180, 1985.

H. J. G. Draaisma, W. J. M. de Jonge, and F. J. A. den Broeder, "Magnetic Interface anisotropy in Pd/Co and Fe/Pd multilayers," J. Magn. Magn. Mater., vol. 66, pp. 351-355, 1987.

P. F. Carcia, "Perpendicular magnetic anisotropy in Pd/Co and Pt/Co thin-film layered structures," J. Appl. Phys., vol. 63 (10), pp. 5066-5073, 1988.

N. Sato, "Crystallographic structure and magnetism of Co-Pd and Co-Pt films with an artificially layered structure," J. Appl. Phys. vol. 64 (11) pp. 64246433, 1988.

3. P. F. Carcia, M. Reilly, W. B. Zeper, and H. W. van Kestern, "Dielectric enhancement layers for a Pt/Co multilayer magneto-optical recording medium," Appl. Phys. Lett., vol. 58 (2), pp. 191-193, 1991.

4. W. B. Zeper, F. J. A. M. Greidanus, P. F. Carcia, and C. R. Fincher, "Perpendicular magnetic anisotropy and magneto-optical Kerr effect of vapor-deposited Co/Pt-layered structures J. Appl. Phys., vol. 65 (12), pp. 4971-4975, 1989.

5. Y. Ochiai, S. Hashimoto, and K. Aso, "Co/Pt and Co/Pd ultrathin multilayered films as new magneto-optical recording materials," IEEE Trans. Magn., vol. 25 (5) pp. 3755-3757, 1989.

W. B. Zeper, F. J. A. M. Greidanus, and P. F. Carcia, "Evaporated Co/Pt layered structures for magneto-optical recording", IEEE Trans. Magn., vol. 25 (5), pp. 3764-3766, 1989.

W. B. Zeper, H. W. van Kestern, and P. F. Carcia, "Co/Pt multilayers for magneto-optical recording," Adv. Mater., vol.3 (7/8), pp. 397-399, 1991.

6. D. Weller and W. Reim, "Magneto-optical spectroscopy of RE/TM alloys and TM/Co multilayers," Mat. Res. Soc. Symp. Proc. Vol. 232, pp. 71-84, 1991.

7. S. Hashimoto, and Y. Ochiai, "Co/Pt and Co/Pd multilayers as magneto-optical recording materials," J. Magn. Magn. Mater., vol. 88, pp. 211-226, 1990.

S. Hashimoto, H. Matsuda, and Y. Ochiai, "Recording experiments in magneto-optical disks using ultrthin Co/Pt and Co/Pd media," Appl. Phys. Lett., vol. 56 (11), pp. 1069-1071, 1990.

P. F. Carcia, S. I. Shah, and W. B. Zeper, "Effect of energetic bombardment on the magnetic coercivity of sputtered Pt/Co thin-film multilayers," Appl. Phys. Lett., vol. 56 (23), pp. 2345-2347, 1990.

8. F. J. A. M. Greidanus, W. B. Zeper, F. J. A. den Broeder, W. F. Godlieb, and P. F. Carcia, Appl. Phys. Lett., vol. 54 (24), pp. 2481-2483, 1989.

9. P. He, W. A. McGahan, J. A. Woolam, F. Sequeda, T. McDaniel, and H. Do, "Magneto-optical Kerr effect and perpendicular magnetic anisotropy of evaporated and sputtered Co/Pt multilayer structures," 4021-4028, 1991.

10. C. H. Lee, R. F. C. Farrow, C. J. Lin, E. E. Marinero, and C. J. Chien, "Molecular-beam-epitaxial growth and magnetic properties of Co-Pt superlattices oriented along the [001], [110], and [111] axes of Pt," Phys. Rev. B, vol. 42 (17), PP. 11384-11387, 1990.

11. K. Nakamura, S. Tsunashima, S. Iwata, and S. Uchiyama, "Magneto-optical properties of PdCo based multilayered films," IEEE Trans. Magn., vol. 25 (5), pp. 3758-3760, 1989, and S. Tsunashima, *et al.*, "Perpendicular magnetic anisotropy of Pd-Co alloy films and related multilayers," *op. cit.* pp. 3761-3763;

B. N. Engel, M. H. Wiedmann, R. A. Van Leeuwen, and C. M. Falco, "Influence of structure on the magnetic anisotropy of Co/Pd(011) epitaxial superlattices," Appl. Surf. Sci. (unpublished preprint), and B. N. Engel, C. D. England, R. A. Van

Leeuwen, M. H. Wiedmann, and C. M. Falco, "Interface magnetic anisotropy in epitaxial superlattices," Phys. Rev. Lett., vol. 67 (14), pp. 1910-1913, 1991;

Y. Maeno, H. Yamane, K. Sato, and M. Kobayashi, "Magnetic properties of multiple-structure multilayered Co/Pd films", Appl. Phys. Lett., vol. 60 (4) pp. 510-511, 1992;

S. T. Purcell, H. W. van Kesteren, E. C. Cosman, W. B. Zeper, and W. Hoving, "Magnetic properties of ultrathin epitaxial Co films on a Pd(111) single crystals," J. Appl. Phys., vol. 69 (8), pp. 5640-5642, 1991, and S. T. Purcell, H. W. van Kesteren, E. C. Cosman, and W. Hoving, "Structural and magnetic studies of ultrathin epitaxial Co deposited on a Pd(111) single crystal,", J. Magn. Magn. Mater., vol. 93, pp. 25-30, 1991.

12. C. D. England, D. C. Person, W. R. Bennett, W. Reim, and C. M. Falco, "Magneto-optic properties of Cu/Co and Pd/Co multilayers," Mat. Res. Symp. Proc. Vol. 150, pp. 103-108, 1989.

13. E. R. Moog, J. Zak, and S. D. Bader, "Kerr effect from Pt/Co superlattices and the role of the magneto-optic activity of Pt," J. Appl. Phys., vol. 69 (2), pp. 880-885, 1991.

14. E. R. Moog, J. Zak, and S. D. Bader, "Analysis of Kerr rotation from Cu/Co, Pd/Co, and Pt/Co superlattices," J. Appl. Phys., vol. 69 (8), pp. 4559-4561, 1991.

15. R. H. Victora and J. M. MacLaren, "Magnetic and electronic properties of Co/Pd superlattices," SPIE, vol.1499, pp. 378-381, 1991, and "Calculated magnetic and electronic properties of Co/Pd superlattices," J. Appl. Phys. vol. 68 (8), pp. 5652-5654, 1991.

16. H. Ebert, S. Ruegg, G. Schütz, R. Wienke, and W. B. Zeper, "Magnetic properties of Co/Pt-multilayers," J. Magn. Magn. Mater., vol. 93, pp. 601-604, 1991.

17. J. Zak, E. R. Moog, C. Liu, and S. D. Bader, "Universal Approach to Magneto-optics," J. Magn. Magn. Mater., vol. 89, pp. 107-123, 1990; and "Magneto-optics of multilayers with arbitrary magnetization directions," Phys. Rev. B, vol. 43 (8), pp. 6423-6429, 1991.

18. J. Zak, E. R. Moog, C. Liu, and S. D. Bader, "Elementary formula for the magneto-optic Kerr effect from model superlattices," Appl. Phys. Lett., vol. 58 (11), pp.1214-1216, 1991.

19. CRC Handbook of Chemistry and Physics, 60th Edition (CRC, Boca Raton, 1988-89) pp. E-387-E-402.

20. G. S. Krinchik and V. A. Artemev, "Magneto-optical properties of Ni, Co, and Fe in the ultrviolet, visible and infrared parts of the spectrum," Sov. Phys. JETP, vol. 26 (6), pp. 1080-1085, 1968.

21. E. R. Moog, S. D. Bader, and J. Zak, "Role of the substrate in enhancing the magneto-optic response of ultrthin films: Fe on Au," Appl. Phys. Lett., vol. 56 (26), pp. 2687-2689, 1990.

22. J.E. Mattson, M.E. Brubaker, C.H. Sowers, M. Conover, Z. Qiu, and S.D. Bader, "Temperature Dependence of the Magnetoresistance of Sputtered Fe/Cr Superlattices," Phys. Rev. B, vol. 44 (17), pp. 9378-9384, 1991.

23. M. E. Brubaker, J. E. Mattson, C. H. Sowers, and S. D. Bader, "Oscillatory interlayer magnetic coupling of sputtered Fe/Mo superlattices," Appl. Phys. Lett., vol. 58 (20), pp. 2306-2308, 1991.

M. E. Brubaker, E. R. Moog, C. H. Sowers, J. Zak, and S. D. Bader, "Transverse magneto-optic Kerr effect in ultrathin films," J. Magn. Magn. Mater., vol. 103, pp. L7-L12, 1992.

24. J. E. Mattson, C. H. Sowers, A. Berger, and S. D. Bader, "Magnetoresistivity and oscillatory interlayer magnetic coupling of sputtered Fe/Nb superlattices," unpublished preprint.

25. Z. Q. Qiu, J. Pearson, and S. D. Bader, "Additivity of the magneto-optic Kerr signal in ultrathin Fe(110)/Ag(111) superlattices,", Phys. Rev. B, vol. 45, 1 April, 1992 (in press).

26. Z. Q. Qiu *et al.* (unpublished).

27. U. Gradmann, "Surface Magnetism," J. Magn. Magn. Mater., vol. 100, pp.481-496, 1991.

28. S. D. Bader, "SMOKE," J. Magn. Magn. Mater., vol. 100, pp.440-454, 1991; and references cited therein.

29. S. D. Bader, "Thin film magnetism," Proc. IEEE, vol. 78 (6), pp. 909-922, 1990; and "Magneto-optical studies of ultrathin ferromagnetic films," Ultramicroscopy, 1992 (in press).

FIGURES

Fig. 1. Experimental (top panel) and simulated (bottom panel) polar Kerr rotations for bulk Co (solid curve) and for Co/Pt superlattices on Si. The experimental data are from Ref. 4. The superlattice compositions are $[Co(20.2Å)/Pt(17.7Å)]_{14}$, $[Co(9.2Å)/Pt(17.4Å)]_{19}$, $[Co(4.5Å)/Pt(17.7Å)]_{22}$, and $[Co(2.4Å)/Pt(17.4Å)]_{25}$.

Fig. 2. Polar Kerr simulations for a Co/Pt superlattice with and without ZnS coatings and for bulk Co, as described in Ref. 13. The superlattice is $[Co(4.1\ Å)/Pt(19\ Å)]_{25}$ on a Pt substrate.

Fig. 3. Experimental (left panels) and simulated (right panels) longitudinal Kerr ellipticities of an Fe film and of Fe(110)/Ag(111) superlattices. The data in the top panels are plotted *vs* total Fe/Ag film thickness, while that in the bottom panels are plotted for only the total Fe thickness in the film. The fact that the data in the bottom panels all initially follow the same straight line is a manifestation of the magneto-optic additivity law in the ultrathin limit.

Fig. 4. Thickness dependence of the Kerr intensity, which is the height of the Kerr loop in remanence (left panels), and coercivities (right panels) for epitaxial Fe films grown on the indicated single-crystalline substrates. The vertical bars labelled d_c identify the critical thickness values at which the easy axes of magnetization reorient from initially being vertical to being in-plane for the thicker films. The Fe thicknesses are measured in monolayers (ML).

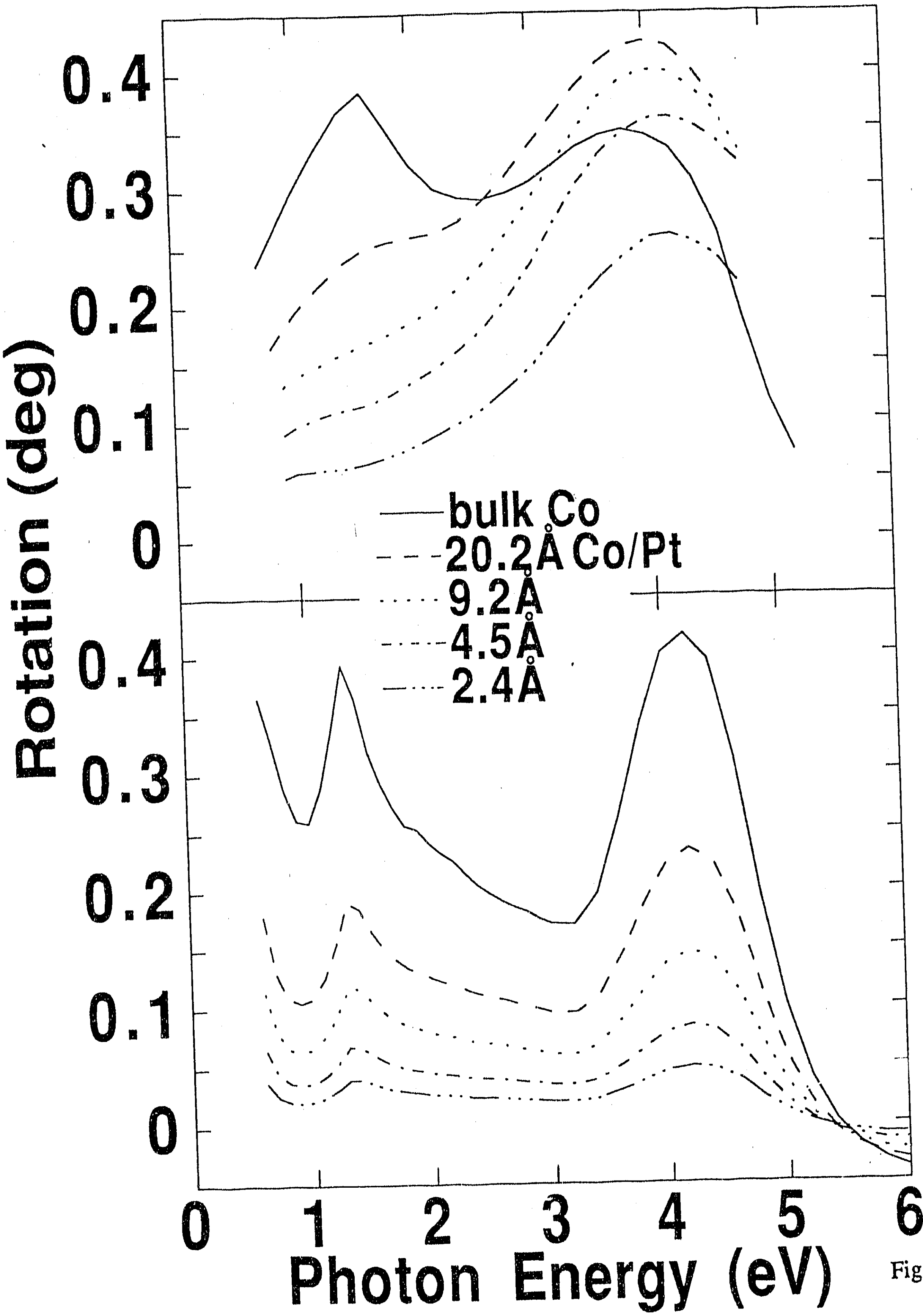
Rotation (deg)
0.4
0.3
0.2
0.1
0
bulk Co
20.2Å Co/Pt
9.2Å
4.5Å
2.4Å
0
1
2
3
4
5
6
Photon Energy (eV)

Figure 1

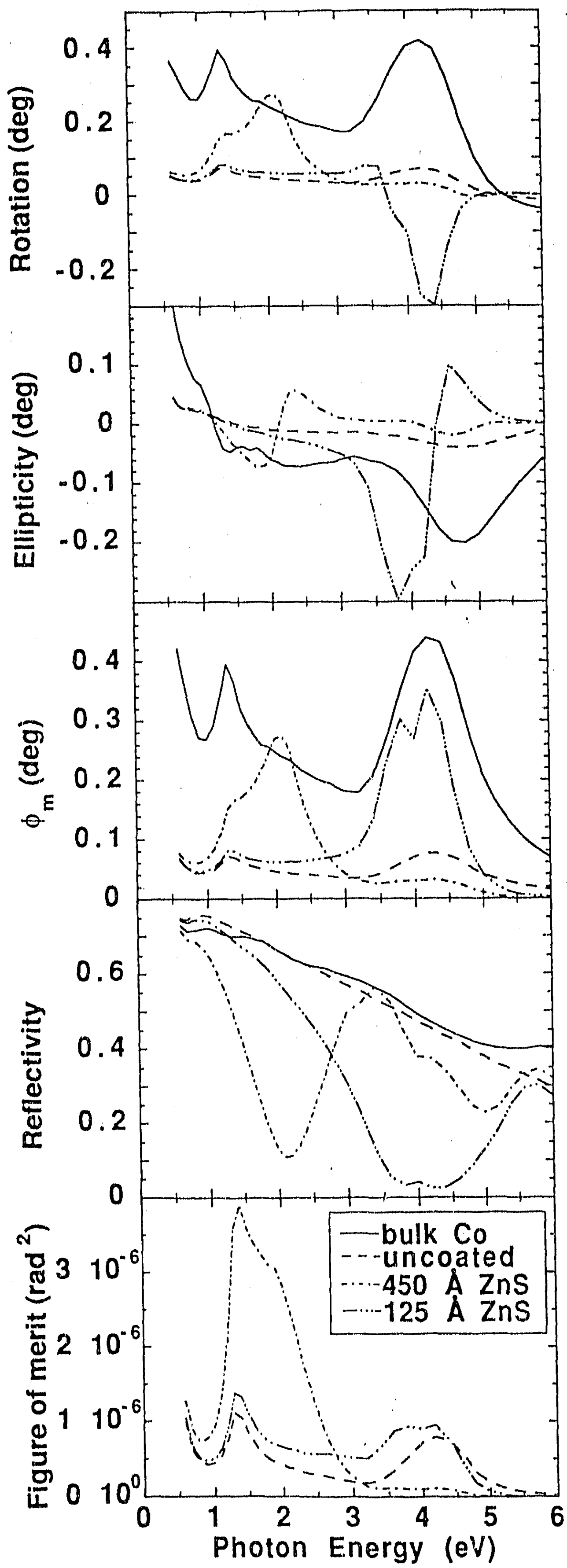
Rotation (deg)
0.4
0.2
0
-0.2
Ellipticity (deg)
0.1
0
-0.1
-0.2
ϕ_m (deg)
0.4
0.3
0.2
0.1
0
Reflectivity
0.6
0.4
0.2
0
Figure of merit (rad^2)
3 10^{-6}
2 10^{-6}
1 10^{-6}
0 10^{0}
bulk Co
uncoated
450 Å ZnS
125 Å ZnS
0
1
2
3
4
5
6
Photon Energy (eV)

Figure 2

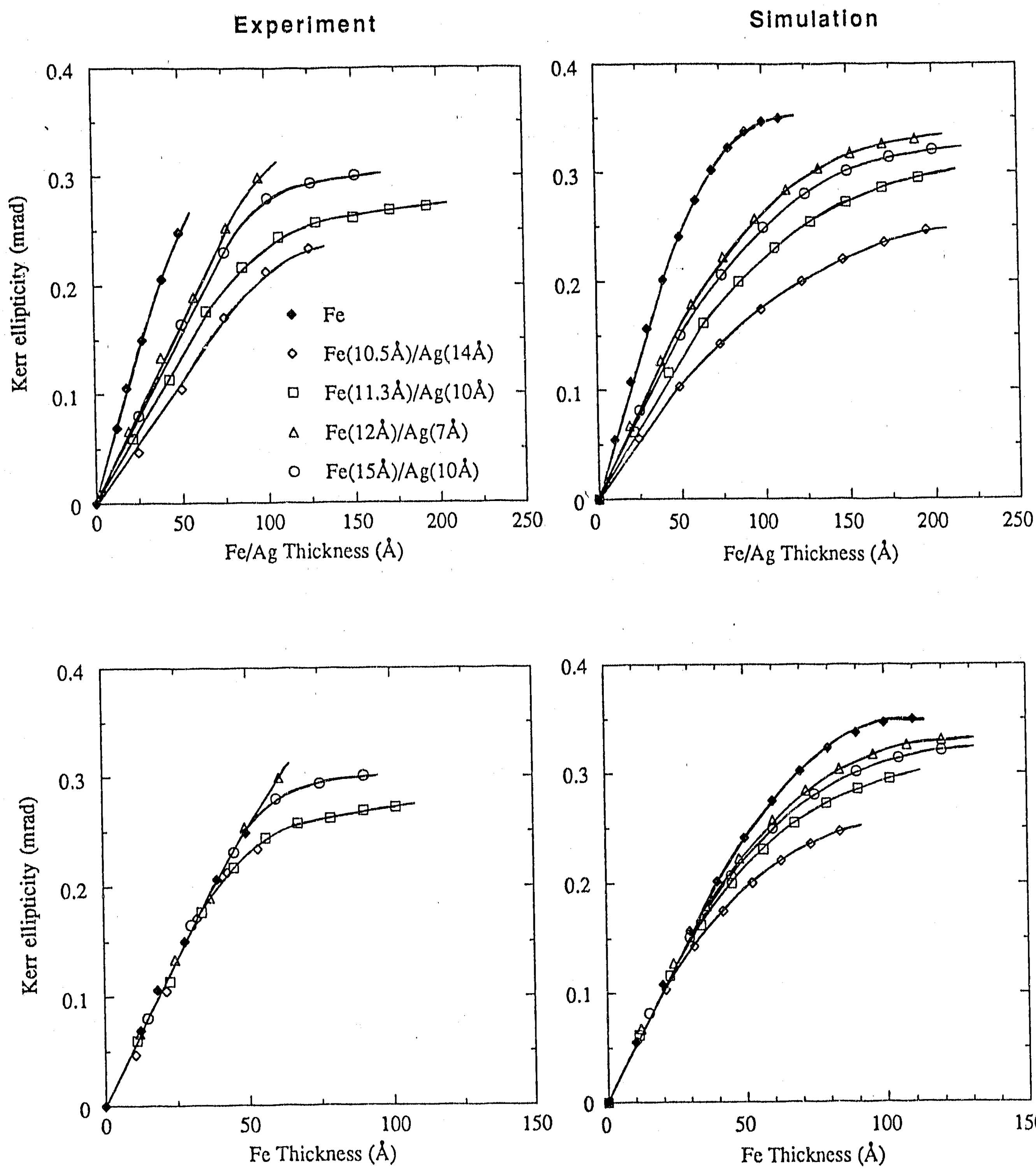

Experiment
Simulation
Kerr ellipticity (mrad)
Fe/Ag Thickness (Å)
Fe
Fe(10.5Å)/Ag(14Å)
Fe(11.3Å)/Ag(10Å)
Fe(12Å)/Ag(7Å)
Fe(15Å)/Ag(10Å)
Fe Thickness (Å)

Figure 3

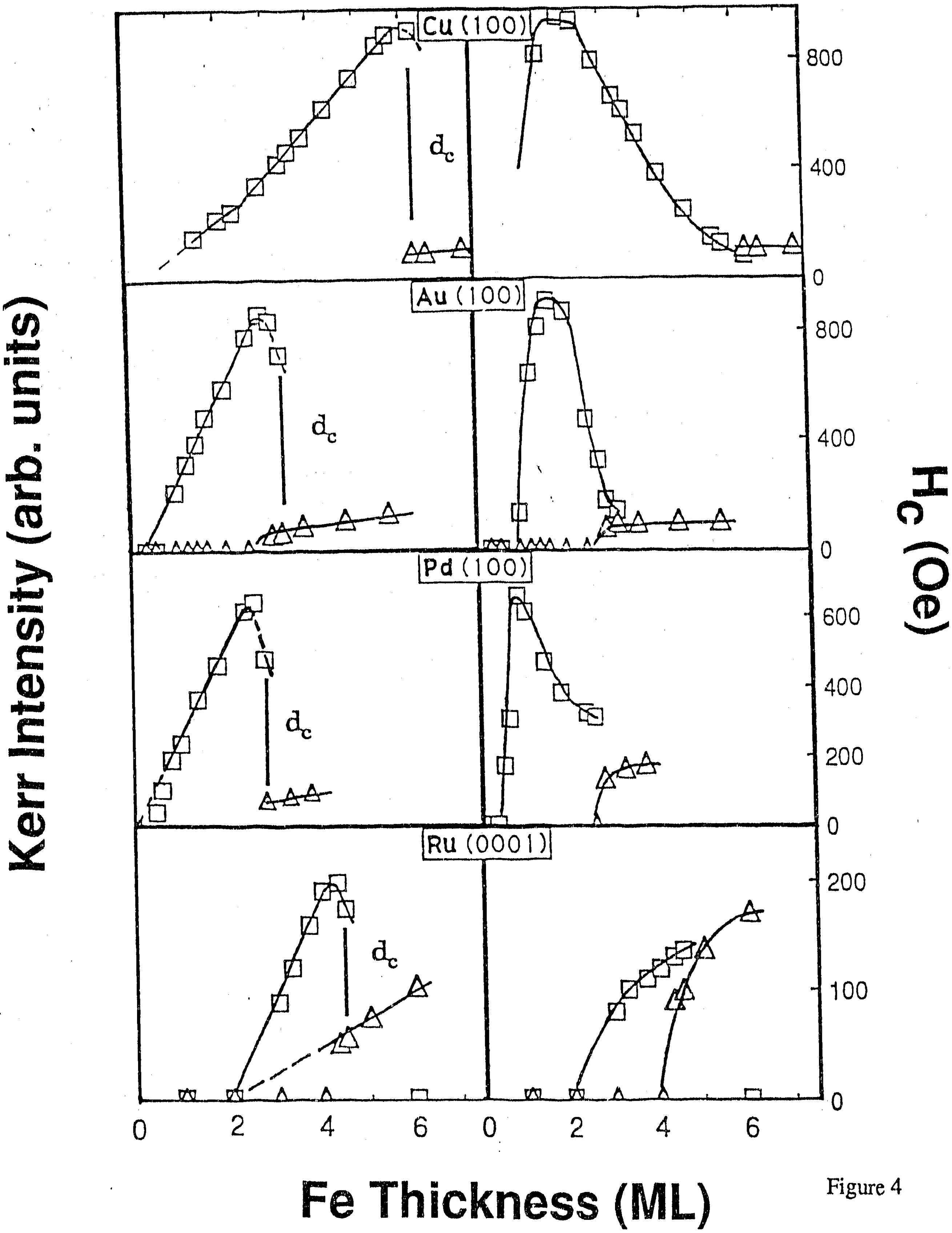

Cu (100)
Au (100)
Pd (100)
Ru (0001)
d_c
Kerr Intensity (arb. units)
H_c (Oe)
Fe Thickness (ML)
0
2
4
6
800
400
600
200
100

Figure 4

DATE
FILMED
5/01/92